Theor Chem Acc (1997) 97:67–71

Theoretical
Chemistry Accounts

Corannulene-based fullerene fragments $C_{20}H_{10}$-$C_{50}H_{10}$: when does a buckybowl become a buckytube?

Kim K. Baldridge[1], **Jay S. Siegel**[2]

[1] San Diego Supercomputer Center, P.O. Box 85608, San Diego, CA 92186-9784, USA
[2] Department of Chemistry, University of California-San Diego, La Jolla, CA 92093-0358, USA

Received: 14 February 1997 / Accepted: 6 May 1997

Abstract. An ab initio study of the structural and physical properties of fullerene fragments based on corannulene shows a distinct defining point between bowl and tube-like character.

Key words: Fullerene fragments – Ab initio – Density functional – Corannulene – Bucky tube

The introduction of a pentagon to a tessellation of hexagons causes warping (bowling) of the surface, and, if 12 pentagons are cooperatively arranged, a closed surface is obtained [**1**]. Chemically, buckminsterfullerene (**1**) [2] and corannulene (**2**) [3, 4] express these extremes. When only six pentagons are added to the motif, it would seem logical that a hemisphere results, to which hexagons could be added forming a capped tube. Such structures represent the minimalist bucky tube motif [5, 6], a family of carbon-rich structures with technological promise [7–11]. Because curvature in graphitic networks alters chemical properties such as dipole moment, ionization potential, and metal binding, the question arises: when does a buckybowl [12, 13] become a buckytube?

Despite the enormous power of chemical synthesis [14], corannulene-based fullerene fragments $C_{30}H_{10}$-$C_{50}H_{10}$ (**3**–**5**) are presently not to be had. As well, these structures have proven a difficult computational challenge; low level computational methods have proven to be ambiguous for quantitative information [15–17], and only corannulene has been treated at correlated levels with promising results [18–20]. Until recent advances in supercomputer hardware, ab initio prediction of the electronic structure of **2**–**5** at double-ζ plus polarization quality and beyond, SCF or correlated methods, would not have been feasible. Following the lead of Jan Almlöf [21–25], we have capitalized on these newer technologies to tackle computational problems exceeding 1000 basis functions (1 kiloBoys or 1 Pople) [26].

Correspondence to: K. Baldridge

Structural computations of the series **1**–**5** were performed at RHF/DZV(2*d*,*p*)[27] using direct [28] SCF methods within the T3E parallel version of GAMESS [29], with select density functional theory, B3PW91/DZ(*d*,*p*), computations on **2**–**4**, using GAUSSIAN94 [30], to uncover effects of dynamic electron correlation. From the fully optimized structures, chemical and physical properties such as ionization potential (Koopmans Theorem) [31, 32] dipole moment, bond localization, and surface curvature (carbon pyramidalization) [33–35] were derived. More extensive computations on the smaller buckyfragments were performed to determine effects of basis set and correlation. These include RHF/DZ(2*df*,2*p*), B3PW91/DZ(2*d*,*p*), and MP2[36]/cc-pVDZ[37] levels of theory. The hybrid DFT methods employ Becke's three parameter hybrid method [38] with the correlation functional of Perdew/Wang91[39] (B3PW91).

The most striking feature in the series **2**–**5** is the increasing bowl depth and surface curvature (Figs. 1, 2). Using the POAV method of Haddon, [33–35, 40] one can assign a pyramidalization value at each carbon. The POAV values for a flat polynuclear aromatic hydrocarbon (PAH) like coronene, the highly symmetrical buckminsterfullerene, the equatorial belt of C_{70}, and a cylindrical benzenoid belt, are 90°, 102°, 99°, and 96°, respectively [35]. Unlike these standards, bowls and capped tubes have variable pyramidality at carbon depending on the position. Because of the conical c_5v symmetry of **2**–**5**, one can define concentric rings of carbons with identical POAV angles. The progression of POAV angle value from the cap-ring (ring 1) to the rim-ring (ring n) is a characteristic of the topography (Table 1). In **2**, the cap pyramidality is similar to the belt region of C_{70}, but already in **3** the cap carbons are essentially as pyramidal as those in C_{60}. By the time one gets to **5**, a pattern of almost constant curvature appears for the lower ring numbers, with the rim ring and ring (n−1) more belt-like. Extension of hexagons onto **5** could continue without substantial change in pyramidality of these limiting carbons, thus pointing to an obvious definable transition between bowl and tube structure. Another structural feature is the angle be-

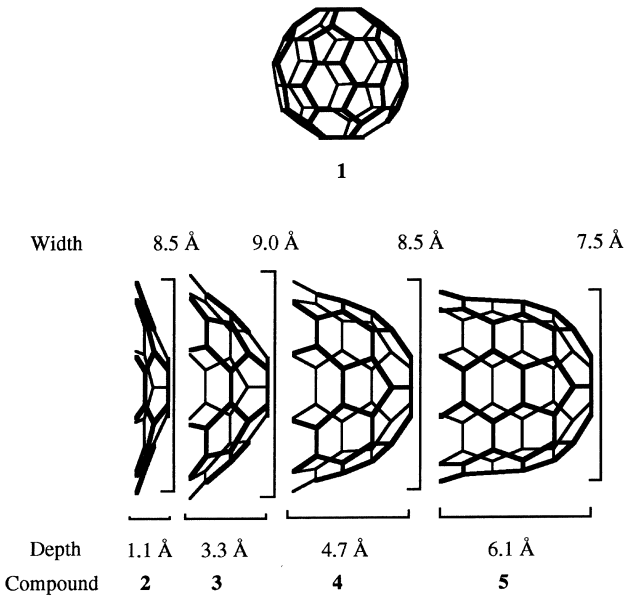

Fig. 1. Nested fullerene fragments showing increasing bowl depth and surface curvature

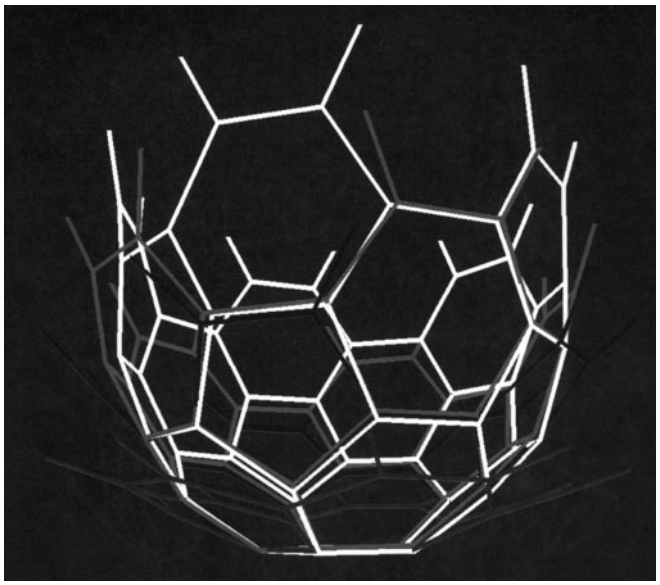

Fig. 2. Nested fullerene fragments

tween the plane of the cap and that of the side near the rim. The value of this angle would be 0° for a flat structure and 90° for a tube. Indeed, **5** has a cap-to-side interplane angle of 86°, consistent with **5** being tube-like. But how do these form features track with other properties?

The central 6-membered ring of flat coronene has a benzenoid geometry with spoke bonds (1.42 Å) essentially equal to the hub bond lengths. (1.41 Å) [41]. The 6-membered ring of bowl-shaped **2** displays differing bond lengths and takes on the [5]radialene motif characteristic of **1**. A bond length localization parameter of the [5]radialene motif can be defined as d(hub) – d(spoke) = delta. A plot of delta across the series **2**–**5** shows a rapid increase in delta which levels off for **4** and **5** at the value derived for **1** (Fig. 3). Thus, delta values would indicate a transition around **4** or **5** where the cap has become like **1**, and further annelation will not perturb delta but will simply extend the length of the tube.

One can take a more detailed look at the variation in structure with level of theory, which we do here for the smallest in the series, **2**. Table 2 shows the basic structure parameters for the corannulene as defined in a previous work [19]. In the case of the hub and spoke bonds described above, the SCF values appear to converge on hub = 1.41 and spoke = 1.36, with additional disagreement with experiment associated then with dynamic correlation, which is mostly made up using either the MP2 or hybrid DFT methods. Although less difficult to predict, the flank and rim bonds show similar behavior. Evaluation of delta for each of these methods shows the general trend of SCF methods overestimating the alternation (0.05–6 vs 0.04), and the hybrid DFT methods as well as the MP2 method underestimating the alternation (0.02–3 vs 0.04). This contrast in SCF and correlated methods holds equally for **3**–**5** (cf. Fig. 3).

In the case of flat PAH and closed fullerenes such as **1**, the dipole moment question is symmetry muted, but for bowls and tubes of conical symmetry, dipoles can be quite substantial. It is well known that large polarized type basis sets which include effects of correlation are required to obtain quantitative values of properties such

Table 1. POAV angle for specific carbons in **2**–**5**; ring 1 starts at the base pentagon

Fragment	Ring 1	Ring 2	Ring 3	Ring 4	Ring 5	Ring 6
$C_{20}H_{10}$	98.3	93.5	91.6			
$C_{30}H_{10}$	102.4	98.6	97.2	91.4		
$C_{40}H_{10}$	102.2	101.2	100.4	98.2	93.5	
$C_{50}H_{10}$	102.1	101.9	101.5	100.0	97.0	92.1
C_{60}	101.6					
C_{70}	101.9	101.9	101.4	100.2	98.6	

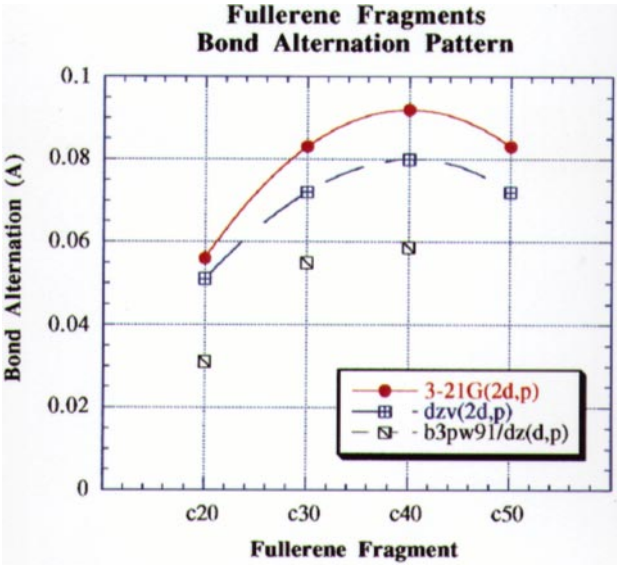

Fig. 3. Bond alternation patterns in fullerene fragments

as dipole moment [42, 43]. Table 2 shows a representative sampling of our investigation of methods for the prediction of dipole moment for corannulene. The SCF as well as hybrid DFT methods converge around 2.1 D for basis sets with significant polarization. The MP2/cc-pvdz predicts a value of dipole which is rather high in comparison. Be that as it may, because no experimental values are yet available for any of our fullerene fragments, and, more importantly, the qualitative trends appear to be preserved across the theories that are more practical for the larger fragments, we look at the DZV (2*d*,*p*) and B3PW91(*d*,*p*) values across the series. A plot of molecular dipole moment from **2**–**5** shows a steep rise from **2**–**4** but a clear plateauing at **4** to **5** (Fig. 4). Assuming a concentration of the charge separation in the cap region, one could imagine a leveling of dipole moment for a tube; little contribution coming from the belt and rim regions. Although we offer no specific reason for this observation, we note that this property correlates well with the structural parameters as a defining point between bowl and tube characters.

Table 2. Structure and property as a function of method for corannulene

Basis set	Hub	Spoke	Flank	Rim	Delta	Dipole
3-21G(2*d*,*p*)	1.415	1.359	1.450	1.370	0.06	2.69
dzv(2*d*,*p*)	1.411	1.360	1.450	1.373	0.05	2.09
dz(2*df*,2*p*)	1.409	1.359	1.448	1.371	0.05	2.07
LDF	1.410	1.380	1.440	1.380	0.03	
BPW91/ 6-31G(*d*)	1.422	1.395	1.451	1.399	0.03	1.84
B3PW91/ dz(*d*,*p*)	1.411	1.381	1.444	1.392	0.03	2.41
B3PW91/ dz(2*d*,*p*)	1.411	1.381	1.444	1.392	0.03	2.10
MP2/ cc-pvdz	1.423	1.401	1.449	1.404	0.02	2.45

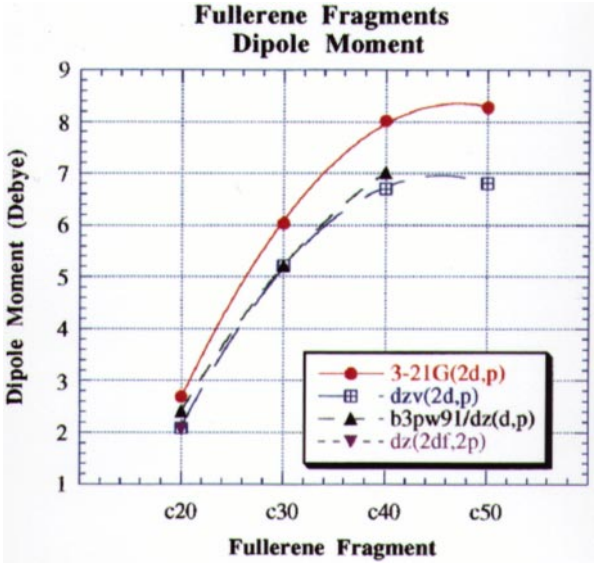

Fig. 4. Dipole moments for fullerene fragments

All graphitic structures, from flat PAHs to spherical **1**, have interesting redox properties such as ionization potential (IP). Applying Koopmans theorem to **2**–**5** [31,

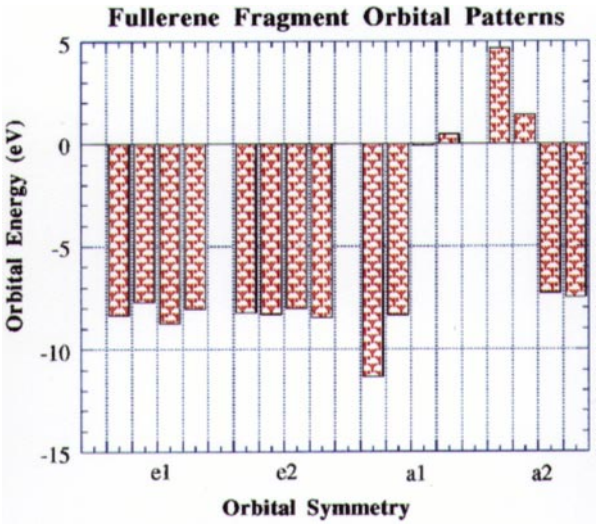

Fig. 5. Orbital energy patterns in fullerene fragments

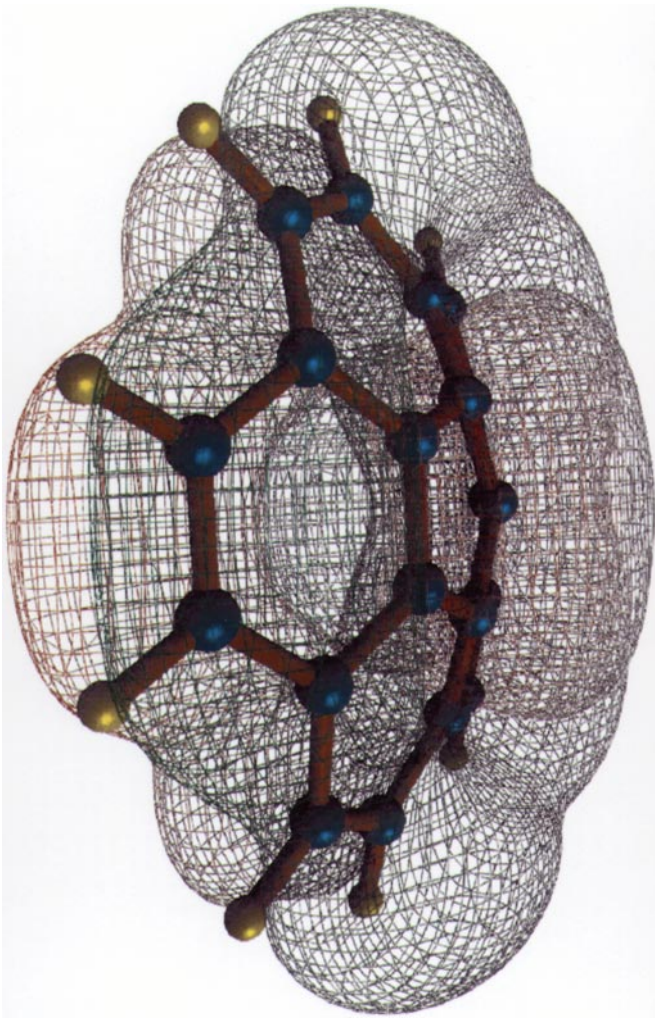

Fig. 6. A1 molecular orbital for corannulene

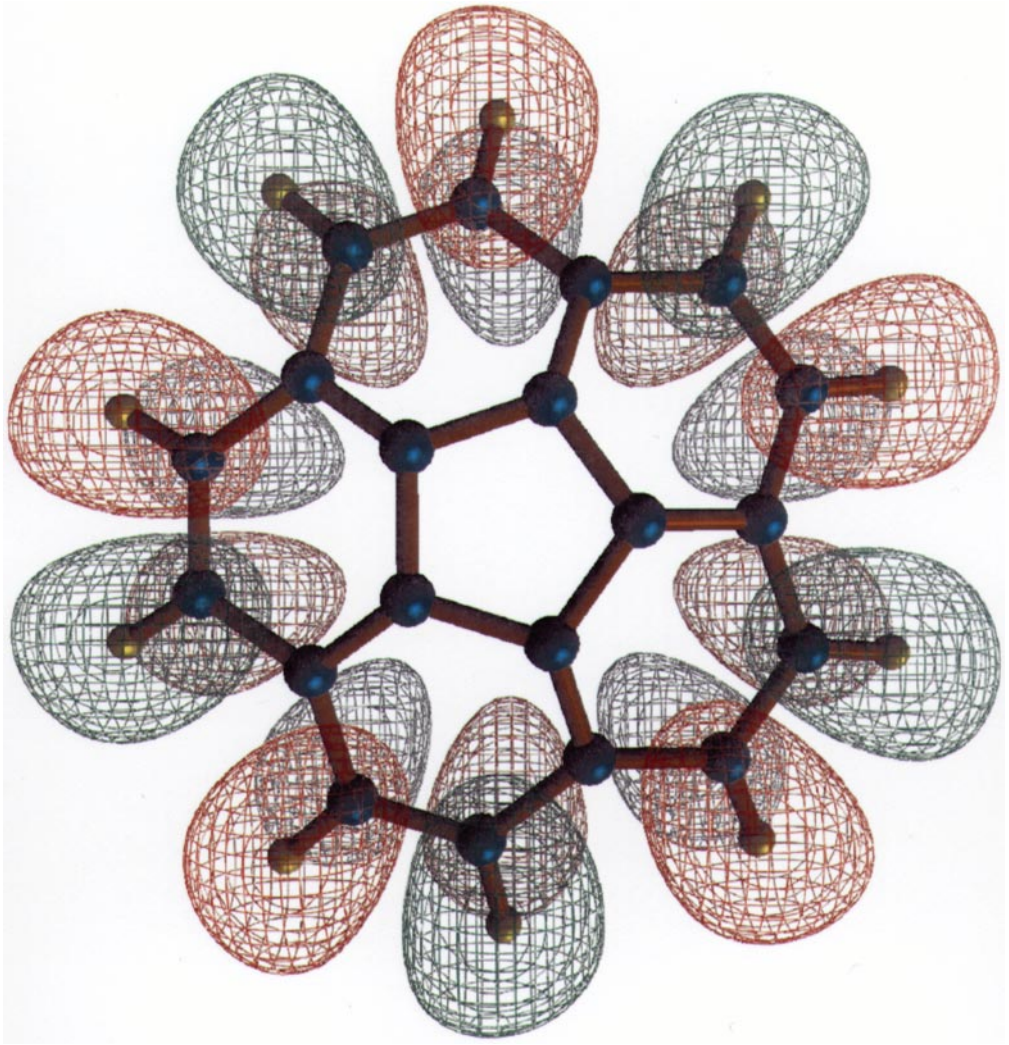

Fig. 7. A2 molecular orbital for corannulene

32], the IP can be approximated. Across the series, the IP varies in an irregular way. This lack of a defining condition between bowls and tubes was initially puzzling; however, a deeper look at the orbital rankings among the first few occupied and virtual orbitals (Fig. 5) shows a perturbation trend in which the orbitals of "a" symmetry (Figs. 6, 7) were strongly shifted compared with the pairwise degenerate "e" sets. The totally symmetric a1 orbital is buried at HOMO-6 in **2**, raises over 2 eV to HOMO-4 in **3**, enters the virtual realm as the LUMO in **4**, and levels off in **5**. The orbital of a2 symmetry complements the behavior of a1. In **2**, a2 is a high lying virtual (LUMO + 6) that drops to LUMO + 2 in **3**, becomes the HOMO for **4**, and levels off there for **5**. Thus, the irregularity of the IP across the series can be attributed to a change in HOMO symmetry, and a symmetry constant analysis of orbital energies shows a defining point around **4** and **5** for the bowl-to-tube transition. Another interesting feature of this change in HOMO/LUMO symmetry is that tubes will be 2-electron donors/acceptors, bowls will be 4-electron donors/acceptors, and C_{60} is a 6-electron donor/acceptor.

Conclusions

From a structural view point, in conjunction with some simple chemical properties, we feel that a reasonable answer to the title question is that $C_{50}H_{10}$ ends the bowl regime, and $C_{40}H_{10}$ begins the tube regime, with some overlap in the transition. The leveling off of the few chemical and physical properties we studied here raises the general question of which properties will and will not be affected by extended tube length. From a synthetic chemists perspective, many of the desired features of a bucky tube may be met through $C_{50}H_{10}$ and derivatives, thus giving great focus to $C_{50}H_{10}$ as a synthetic target for materials design. We hope that such conclusions demonstrate the incredible synergy to be had between modern computational chemistry and designed chemical synthesis. Jan Almlöf certainly had this vision and saw its power early on; the path he sought is clearly being paved, but his perspective will be sorely missed.

Acknowledgements. This work is supported by the US National Science Foundation (CHE9628565 and ASC-02827). We also thank

the San Diego Supercomputer Center for supercomputer support via the grandchallenge/MAC program.

References

1. Beck A, Bleicher MN, Crowe D (1969) Excursions into mathematics. Worth, New York
2. Hirsch A (1994) Chemistry of Fullerenes, 28:79–87
3. Siegel JS, Seiders TJ (1995) Chem Br 31:313–316
4. Scott LT (1996) Pure Appl Chem 68:291–300
5. Balaban AT (1996) Bull Soc Chim Belg 105:383–389
6. Zhen-Ping Z, Yong-Da G (1996) Carbon 34:173–178
7. Dai HJ, Hafner JH, Rinzler AG, Colbert DT, Smalley RE (1996) Nature 384:147–150
8. Cahill PA, Rohlfing CM (1996) Tetrahedron 52:5247–5256
9. Dravid VP, Lin X., Wang Y, Wang XK, Yee A, Ketterson JB, Chang RPH (1993) Science 259:1601–1604
10. Wang XK, Lin XW, Song SN, Dravid VP, Ketterson JB, Chang RPH (1995) Carbon 33:949–958
11. Fonesca A, Hernadi K, Nagy JB, Bernaerts D, Lucas AA (1996) J. Mol. Cat. A. Chem 107, 159–168
12. Scott LT, Bratcher MS, Hagen S (1996) J. Am. Chem. Soc. 118:8743–8744
13. Rabideau PW, Sygula A (1996) Accts. of Chem. Res. 29, 235–242
14. Nicolaou KC, Sorenson EJ (1996) Classics in total synthesis, VCH, Weinheim
15. Henderson CC, Rohlfing CM, Assink RA, Cahill PA (1994) Angew Chem. Int Ed. Engl. 33:786
16. Henderson CC, Rohlfing CM, Gillen KT, Cahill PA (1994) Science 264:396
17. Liu RF, Zhou XF, Allinger NL (1994) J. Phys. Org. Chem. 7:551–554
18. Martin JML (1996). Chem. Phys. Lett. 262:97–104
19. Borchardt A, Baldridge KK, Fuchicello A, Kilway K, Siegel JS (1992) J. Am. Chem. Soc. 114:1921
20. Grossman JC, Mitas L, Raghavachari K (1995) Phys. Rev. Lett. 75:3870–3873, and, Taylor PR, Bylaska E, Weare JH, Kawai R Chem.Phys. Lett. 235:558
21. Panas I, Almlöf JE, Feyereisen MW (1991) Int. J. Quant. Chem. 40:797–807
22. Liu JJ, Feyereisen M W, Almlöf JE, Rohlfing C M (1991) Chem. Phys. Lett. 183, 478–82
23. Parasuk V, Almlöf JE, Feyereisen MW (1991) J. Am. Chem. Soc. 113:1049–1050
24. Parasuk V, Almlöf JE (1991) Chem. Phys. Lett. 184:187–190
25. Almlöf JE, Truhlar DG, Lybrand TP (1990) Int. Sci. Rev. 15:252–263
26. We define the unit of a single basis function as a 'Boys', in honor of Professor Samuel Francis Boys who first demonstrated the feasibility of machine-aided computational chemistry; 1000 basis functions we call a 'Pople', in honor of Professor John Pople who first coupled computational ab initio methods to emerging computer technologies in a general way making possible studies of a magnitude we associate as an earmark of Jan Almlöf
27. Dunning TH Jr, Hay PJ (1977) Methods of electronic structure theory, Plenum, New York, pp 1–17
28. Almlöf JE, Taylor PR (1984) In: Dykstra CE (ed) Advanced theories and computational approaches to the electronic structure of molecules. Reidel, Dordrecht
29. Schmidt MW, Baldridge KK, Boatz JA, Elbert ST, Gordon MS, Jensen JH, Koseki S, Matsunaga N, Nguyen KA, Su S, Windus TL, Elbert ST (1993) J. Comp. Chem. 14:1347
30. Frisch MJ, Trucks GW, Schlegel HB, Gill PMW, Johnson BG, Robb MA, Cheeseman JR, Keith TA, Peterson GA, Montgomery JA, Raghavachari K, Al-Laham MA, Zakrzewski VG, Ortiz JV, Foresman JB, Cioslowski J, Stefanov BB, Nanayakkara A, Challacombe M, Peng CY, Ayala PY, Chen W, Wong MW, Andres JL, Replogle ES, Gomperts R, Martin RL, Fox DJ, Binkley JS, DeFrees DJ, Baker J, Stewart JP, Head-Gordon M, Gonzalez C, Pople JA (1994) Gaussian Pittsburgh P
31. Almlöf JE, Roos B, Wahlgren U, Johansen H (1973) J. Elect. Spect. Rel. Phen. 2:51–74
32. Jordan KD, Paddon-Row MN (1992) J. Phys. Chem. 96:1188–1196
33. Haddon RC (1990) J. Am. Chem Soc. 112:3385–3389
34. Haddon RC (1988) Acc. Chem Res. 21:243
35. Haddon RC, Brus L E, Raghavachari K (1986) Chem. Phys. Lett. 131:165–169
36. Dunlap BI, Connolly JWD, Sabin JR (1979) J. Chem. Phys. 71:3396
37. Woon DE, Dunning, TH (1993) Ar. J Chem. Phys. 98:1358
38. Becke, AD (1993) J. Chem. Phys. 98:5648–5652
39. Perdew JP, Wang Y (1992) Phys. Rev. B 45:13244
40. Haddon RC, Elser V (1990) Chem. Phys. Lett. 169:362–364
41. Fawcett JK, Trotter J (1966) Proc. R. Soc. A289, 366
42. Taylor PR (1992) In: Roos B (ed) Lecture Notes in Quantum Chemistry. Springer, Berlin Heidelberg New York, vol. 58
43. Almlöf JE, Helgaker T, Taylor PR (1988) J. Phys. Chem. 92:3029